

# Physicochemical and Electrochemical Characterization of Polycyclopenta[2,1-*b*;3,4-*b'*]dithiophen-4-one as an Active Electrode for Electrochemical Supercapacitors

Florence Fusalba, Naima El Mehdi, Livain Breau, and Daniel Bélanger\*

Département de Chimie, Université du Québec à Montréal, Case Postale 8888, succursale Centre-Ville, Montréal, Québec, Canada, H3C 3P8

Received March 2, 1999. Revised Manuscript Received July 26, 1999

Poly(cyclopenta[2,1-*b*;3,4-*b'*]dithiophen-4-one) (PCDT) has been characterized by several electrochemical and spectroscopic techniques so that it can be used as an active electrode material in electrochemical supercapacitors. This polythiophene derivative was prepared by the electrochemical polymerization of cyclopenta[2,1-*b*;3,4-*b'*]dithiophene-4-one (CDT) from a nonaqueous solution (acetonitrile) containing tetraethylammonium tetrafluoroborate. The range of electroactivity of PCDT in nonaqueous media spans at least 2 V. The doping levels measured by cyclic voltammetry and EDAX were found to be 0.19 and 0.14, respectively, for the oxidized-PCDT. Low-frequency capacitance measurements were made by electrochemical impedance spectroscopy to evaluate the film's ability to store charge. Low-frequency capacitances of about  $\sim 70$  F/g were found for both the p- and n-doped states. Ionic and electronic resistances were established using both a Randles equivalent circuit and the linear transmission line model to analyze the impedance data of electronically conducting polymers. The film morphology was studied by scanning electron microscopy, and photomicrographs revealed an open and porous structure. X-ray photoelectron spectroscopy was employed to evaluate the electronic properties of the polymer. Negatively charged sulfur atoms were only observed in low content probably due to low negative polaron stability and the sensitivity of the polymer to trace amounts of oxygen and water. Nonetheless, the S  $2p^{o-}$  species for the n-doped state has clearly been identified in our study as we present here. A conservative estimate of the doping level was found to be  $\sim 0.06$ . Preliminary galvanostatic charge/discharge cycling experiments indicated an energy density,  $E$ , of about 6 (W h)/kg for the active material with a power density,  $P$ , of 1 kW/kg for an 18 s discharge time. These values are above the midterm requirements fixed by the U. S. Department of Energy for electrochemical supercapacitors ( $E > 5$  (W h)/kg and  $P > 500$  W/kg). A discharge capacity decrease was observed during the first 20 cycles but thereafter the discharge capacity remained constant for the next 80 cycles. Additional work is currently under way to improve the stability of the PCDT-based capacitor since this conducting polymer should be very interesting as an active electrode in electrochemical supercapacitors.

## Introduction

Conducting polymers have attracted a lot of interest in the past two decades primarily because these materials have several applications.<sup>1</sup> One of these applications is as an active electrode material in electrochemical supercapacitors.<sup>2–5</sup> Three types of electrochemical supercapacitors based on conducting polymers have been proposed<sup>2,3</sup> and the motivation for the use of polythiophene derivatives instead of polyaniline or

polypyrrole in such devices stems from the fact that a higher cell voltage can be achieved with the polythiophene as most of these can be n- and p-doped over a potential range of 2–3 V.<sup>6,7</sup> On the other hand, the range of electroactivity of polypyrrole and polyaniline spans at most 1 V.<sup>5,8</sup> Therefore, we have evaluated several thiophene derivatives as precursors for various electrochemical supercapacitors.<sup>9,10</sup> Unfortunately, the high cell voltage which can be achieved with polythiophenes may be counterbalanced by a high sensitivity of the n-doped form to traces of water and oxygen since a high cathodic potential (ca.  $-2$  V vs Ag/Ag<sup>+</sup>) is typically required to n-dope polythiophene.<sup>2,6,7</sup> As an alternative to these polymers, narrow band gap poly-

\* Author to whom all correspondence should be sent. E-mail: belanger.daniel@uqam.ca.

(1) (a) Novak, P.; Muller, K.; Santhanam, K. S. V.; Hass, O. *Chem. Rev.* **1997**, *97*, 207. (b) Miller, J. S. *Adv. Mater.* **1993**, *5*, 587. (c) Miller, J. S. *Adv. Mater.* **1993**, *5*, 671.

(2) Rudge, A.; Davey, J.; Raistrick, I.; Gottesfeld, S.; Ferraris, J. P. *J. Power Sources* **1994**, *47*, 89.

(3) Arbizzani, C.; Mastragostino, M.; Scrosati, B. *Handbook of organic conductive molecules and polymers*; Nalwa, H. S., Ed.; John-Wiley & Sons Ltd.: New York, 1997; Vol. 4, p 595.

(4) Carlberg, J. C.; Ingas, O. *J. Electrochem. Soc.* **1997**, *144*, L61.

(5) Garcia, B.; Fusalba, F.; Bélanger, D. *Can. J. Chem.* **1997**, *75*, 1536.

(6) Roncali, J. *Chem. Rev.* **1992**, *92*, 711.

(7) Roncali, J. *Chem. Rev.* **1997**, *97*, 173.

(8) Garcia, B.; Bélanger, D. *Synth. Met.* **1998**, *98*, 135.

(9) Naudin, E. M.Sc. Thesis Université du Québec à Montréal, 1997, p 152.

(10) Fusalba, F.; Ho, A. H.; Breau, L.; Bélanger, D. Manuscript in preparation.

thiophenes should allow more stable n-doping at less negative potentials but at the expense of cell voltage.

There are several strategies for the reduction of the band gap<sup>7,11</sup> but the main one consists of using a monomer with reduced aromaticity and whose decreased HOMO–LUMO separation can be carried over into its polymer. An example of this would be the low band gap polymer introduced by Ferraris and Lambert,<sup>12,13</sup> polycyclopenta[2,1-*b*;3,4-*b'*]dithiophen-4-one (PCDT), which can be prepared by electrochemical polymerization of the corresponding monomer. Previous studies of PCDT<sup>12–14</sup> by optical spectroscopy and cyclic voltammetry have shown that the potential difference between the threshold for hole injection (p-doping) and electron injection (n-doping) leads to an estimated band gap of ~1.2 eV. In situ IR spectroscopy reported by Beyer et al.<sup>15</sup> confirmed the presence of an electronic absorption band in both states of doping. However, they showed that the intensity of this absorption band for the n-doped state is greatly reduced. They concluded that it is possible for PCDT to undergo n- and p-doping, although the extent of the n-doping is much smaller. This is in contrast with the data reported by others<sup>12–14</sup> in which PCDT exhibited a large degree of n-doping. Beyer et al.<sup>15</sup> have also reported on the electrical properties of PCDT-based diodes. Their results showed that in the solid state, Al/PCDT/Au diodes displayed little or no rectification, although capacitance and loss data showed the strong frequency dispersion characteristic of a Schottky diode.

In this paper, we report the electrochemical synthesis of polycyclopenta[2,1-*b*;3,4-*b'*]dithiophen-4-one and its characterization by cyclic voltammetry, electrochemical impedance spectroscopy, scanning electron microscopy, and X-ray photoelectron spectroscopy. Also presented is the charge/discharge behavior of carbon paper/PCDT-based electrochemical supercapacitors.

## Experimental Section

**Chemicals.** Acetonitrile from Aldrich was either distilled before use or used as is if the acetonitrile was HPLC grade. Cyclopenta[2,1-*b*;3,4-*b'*]dithiophen-4-one, CDT, was synthesized according to procedures previously reported.<sup>15–17</sup> All spectroscopic and physical data for CDT were similar to those reported in the literature.

**PCDT Film Electrodeposition.** The working electrodes were 0.5 cm × 1 cm and 0.010-in.-thick carbon paper (Spectracorp) with a specific surface area of 1–2 m<sup>2</sup>/g. Typically, the weight of the carbon electrode was 0.48 g/cm<sup>2</sup>. Prior to any measurements, the carbon paper electrodes were washed in methanol in an ultrasonic bath for 1–2 min and dried at 50 °C. Platinum foil (0.5 cm × 2.5 cm) was also used as working electrode and was flamed before being washed with CH<sub>3</sub>CN.

(11) Pomerantz, M. *Handbook of Conducting Polymers*, 2nd ed.; Skotheim, T., Elsenbaumer, R. L., Reynolds, J. R., Eds.; Marcel Dekker: New York, 1998; p 277.

(12) Ferraris, J. P.; Lambert, T. L. *J. Chem. Soc., Chem. Commun.* **1991**, 1268.

(13) Lambert, T. L.; Ferraris, J. P. *J. Chem. Soc., Chem. Commun.* **1991**, 752.

(14) Brisset, H.; Thobie-Gautier, C.; Gorgues, A.; Jubault, M.; Roncali, J. *J. Chem. Soc., Chem. Commun.* **1994**, 1305.

(15) Beyer, R.; Kalaji, M.; Kingscote-Burton, G.; Murphy, P. J.; Pereira, V. M. S. C.; Taylor, D. M.; Williams, G. O. *Synth. Met.* **1998**, *92*, 25.

(16) Jordens, P.; Rawson, G.; Wynberg, H. *J. Chem. Soc. C* **1970**, 273.

(17) Wu, X.; Chen, T.; Zhu, L.; Rieke, R. D. *Tetrahedron Lett.* **1994**, *35*, 3675.

The reference electrode was a Ag/Ag<sup>+</sup> (10 mM AgNO<sub>3</sub>, 0.1 M tetrabutylammonium perchlorate in acetonitrile) electrode and a platinum flag (area = 1 cm<sup>2</sup>) served as the counter electrode. The polymer films were grown from a solution containing 10–60 mM of cyclopenta[2,1-*b*;3,4-*b'*]dithiophen-4-one and 1 M tetraethylammonium tetrafluoroborate in acetonitrile. Electropolymerization was performed galvanostatically at a current density of 0.05–0.5 mA/cm<sup>2</sup>. The films were then washed in acetonitrile to remove any soluble species from the film and cycled in a monomer free solution of 1 M tetraethylammonium tetrafluoroborate in acetonitrile between –1.7 and 0.8 V vs Ag/Ag<sup>+</sup>.

**Procedure and Equipment.** The morphology and thickness of the deposited films were observed by scanning electron microscopy, SEM, using a Hitachi model S-5300 microscope. Relative estimates of the atomic content of the film were obtained by using a KeveX Quantum 3600-0388 energy-dispersive (EDS) X-ray analyzer. Photomicrographs and EDAX spectra were taken on various PCDT film-coated carbon papers and platinum electrodes after the following treatments: (i) freshly electrodeposited, (ii) reduced at –1.4 V in 1 M Et<sub>4</sub>NBF<sub>4</sub>/ACN, and (iii) oxidized at 0.4 V in 1 M Et<sub>4</sub>NBF<sub>4</sub>/ACN.

All the films were thoroughly rinsed with CH<sub>3</sub>CN prior to analysis. X-ray photoelectron spectroscopy, XPS, measurements were performed with a VG Escalab 220i-XL system equipped with an hemispherical analyzer and an Al anode (K<sub>α</sub> X-rays at 1486.6 eV) at 10 kV and ~15 mA. The data were obtained at room temperature, and typically the operating pressure in the analysis chamber was below 1 × 10<sup>–9</sup> Torr. XPS spectra were performed on various PCDT films-coated platinum electrode after being: (i) freshly electrodeposited (as-grown), (ii) reduced at –1.4 V in 1 M Et<sub>4</sub>NBF<sub>4</sub>/ACN, (iii) oxidized at 0.4 V in 1 M Et<sub>4</sub>NBF<sub>4</sub>/ACN, and (iv) cycled in 1 M Et<sub>4</sub>NBF<sub>4</sub>/ACN between –1.7 and 0.75 V, stopped and then polarized at –0.5 V.

Precautions were taken to minimize exposure to air and water by using an atmsbag (Aldrich) for sample transfer to the antichamber of the spectrometer. Survey scans in the range of 0–1000 eV were recorded at a pass energy of 100 eV with a step size of 1 eV. Core level spectra were obtained for C 1s, S 2p, F 1s, B 1s, N 1s, and O 1s with a pass energy of 20 eV and a step size of 50 meV. Typically, one to four detailed scans were recorded. Curve fitting of the XPS data was carried out with Origin software (version 5.0). A semiquantitative evaluation of relative atomic surface concentrations was obtained by considering their corresponding sensitivity factors: C 1s (1.0), S 2p<sub>1/2</sub> (0.567), S 2p<sub>3/2</sub> (1.11), F 1s (4.43), B 1s (0.486), N 1s (1.8), and O 1s (2.93). The binding energies were corrected for surface charging by referencing them to the designated hydrocarbon C 1s binding energy as 284.5 eV.

All electrochemical measurements were performed in a glovebox under a dry and N<sub>2</sub> atmosphere, in a closed three-electrode cell. Cyclic voltammetric studies were performed using a potentiostat model 1287 Solartron Electrochemical Interface coupled to a PC with Corrware Software for Windows (Scribner Associates, version 1.4). During the electrochemical measurements, a total geometric area of 1 cm<sup>2</sup> of the two carbon paper faces were exposed to the electrolytic solution. This total area has been used in reporting our results. For example, low-frequency capacitance values are given in farads per squared centimeter (F/cm<sup>2</sup>). For values given versus weight [i.e., farads per gram (F/g) and watt-hour per kilogram ((W h)/kg)], calculations via the weight were obtained for 5 C of the as-grown conducting polymer electropolymerized on a 1 cm<sup>2</sup> carbon paper electrode ( $m_{\text{polymer}} = 0.0045$  g). For the film grown with a charge of 1 C/cm<sup>2</sup>, we assumed a constant polymer growth and the polymer was taken as 5 times smaller (0.0009 g). Electrochemical impedance measurements were performed with a model 1255 Solartron Frequency Response Analyzer coupled to a model 1287 Solartron Electrochemical Interface. Data were collected and analyzed using a PC and Zplot Software for Windows (Scribner Associates, version 1.4). Electrode potential measurements were made over a frequency range of 65 kHz to 0.05 Hz using a 10 mV sine-wave amplitude. The polymer electrode was polarized at the ap-

**Table 1. Effect of the Variation of the Growth Conditions on the Electrochemical Behavior of PCDT**

$Q_{\text{deposited}}$ (C/cm <sup>2</sup> )	[CDT] mM	$i$ (mA/cm <sup>2</sup> )	$E_{\text{stab}}$ (V)	$Q_{\text{ox(p)}}/Q_{\text{red(p)}}^a$ (mC/cm <sup>2</sup> )	$Q_{\text{red(n)}}/Q_{\text{ox(n)}}^a$ (mC/cm <sup>2</sup> )	doping level, $x^b$	
						p	n
0.2	10	0.1	0.73	19/6	12/3	0.10	0.06
	10	1	0.85	17/5	14/5	0.09	0.08
	20	0.1	0.68	29/12	16/3	0.17	0.09
	20	0.5	0.76	32/12	35/14	0.19	0.21
	30	0.1	0.62	6/0.7	4/0.4	0.03	0.02
	30	0.5	0.66	34/19	12/2	0.20	0.06
	50	0.1	0.72	25/18	16/11	0.14	0.09
	50	0.5	0.74	37/21	23/11	0.23	0.13
	60	0.1	0.72	17/12	25/18	0.09	0.14
	60	0.5	0.74	31/9	27/12	0.18	0.18
0.5	20	0.5	0.67	78/67	45/33	0.18	0.10
	10	0.1	0.67	205/147	78/29	0.26	0.18
1	20	0.1	0.85	123/53	101/35	0.14	0.11
	20	0.5	0.73	182/131	208/144	0.22	0.26
	50	0.5	0.65	150/68	56/6	0.18	0.06
5	20	0.5	0.71	312/302	220/231	0.07	0.05

<sup>a</sup> Scan rate for 0.2 C/cm<sup>2</sup> is 100 mV/s; 1 C/cm<sup>2</sup> is 10 mV/s; 0.5 and 5 C/cm<sup>2</sup> is 25 mV/s. <sup>b</sup> Calculated from  $x = (Q_{\text{CV}}/Q_{\text{deposited}})/(1 - (Q_{\text{CV}}/Q_{\text{deposited}}))$ , with  $Q_{\text{CV}} = Q_{\text{ox(p)}} \text{ or } Q_{\text{red(n)}}$  and assuming a polymerization efficiency of 100%.

appropriate potential for about 50 s before the impedance measurements were taken to ensure that the polymer film electrode had reached equilibrium.

The charge–discharge experiments were performed with 2 PCDT-coated carbon paper electrodes separated by about 0.5 cm and placed in a flooded electrolyte cell. A Ag/Ag<sup>+</sup> reference electrode was also used to monitor the potentials of each electrodes during cycling. Following polymer growth, the potential of each electrodes was set at about –0.2 V versus Ag/Ag<sup>+</sup> and the capacitor was charged at 2 mA/cm<sup>2</sup> from 0 to 2 V. To ensure that the capacitor is fully charged, the cell voltage was maintained at 2 V for 100 s and the discharge was carried out at 2 mA/cm<sup>2</sup>.

## Results and Discussion

**Cyclic Voltammetry, CV.** When PCDT was galvanostatically electropolymerized at a current density of 0.5 mA/cm<sup>2</sup>, a stabilization potential ( $E_{\text{stab}}$ ) of about 0.73 V  $\pm$  0.03 V was obtained (see Table 1). Typical cyclic voltammograms of PCDT in 1 M Et<sub>4</sub>NBF<sub>4</sub>/acetonitrile are shown in Figure 1 and are characterized by two sets of broad redox waves. The first are centered at about 0.3 V and are associated with the p-doping process whereas the n-doping redox waves are centered at ca. –1.3 V. The shape of these CVs is similar to that reported by Lambert and Ferraris<sup>12,13</sup> but differs from that of Brisset et al.<sup>14</sup> In contrast, the last group found the waves for the n-doping process to be sharp and their intensities were higher than those for the p-doping ones. Therefore, our results as well as those of Lambert and Ferraris<sup>12,13</sup> and Brisset et al.<sup>14</sup> indicate that PCDT can be n-doped, whereas Beyer et al.<sup>15</sup> reported that the extent of n-doping was much smaller than that of the p-doping. The anodic peak potential for the p-doping process and the cathodic peak potential for the n-doping wave were found to be similar to those reported by Lambert and Ferraris<sup>12,13</sup> and Brisset et al.<sup>14</sup> The slight difference may be explained by the differing conditions used for the electrochemical growth of the polymer. In contrast to the results of Lambert and Ferraris,<sup>13</sup> the anodic peak current is a linear function of the square root of scan rate, indicating an ionic diffusion-limited process.<sup>18</sup> This could be explained by the fact that a thicker film was used in our work (1 C/cm<sup>2</sup>). Finally, it should be noticed that CVs with different cycling limits

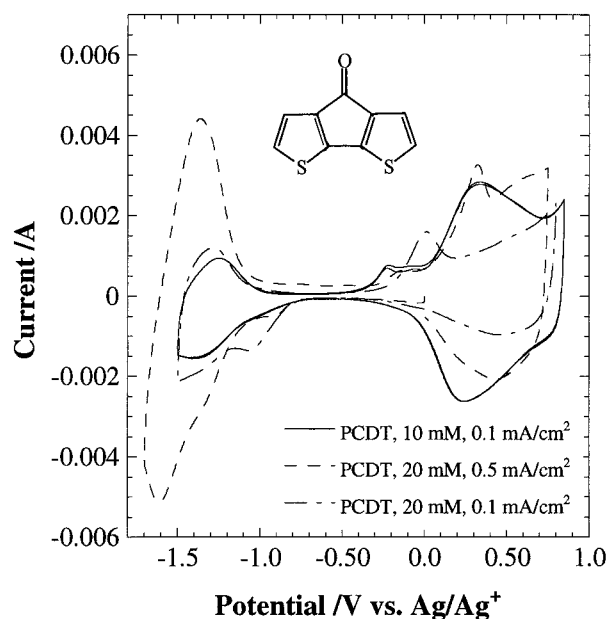


**Figure 1.** Cyclic voltammograms of PCDT ( $Q_{\text{deposited}} = 1$  C/cm<sup>2</sup>) on carbon paper electrode in 1 M Et<sub>4</sub>NBF<sub>4</sub> in acetonitrile, for various growth conditions. Scan rate: 10 mV/s. Structure of the CDT Monomer is given.

are shown in Figure 1. This allows for the observation of the reduction peak for n-doping on one hand and an onset of anodic current, which is presumably linked to PCDT irreversible degradation, on the other hand.

The CVs of Figure 1 also show cathodic and anodic prepeaks around –1 and –0.1 V, respectively, for the n- and p-doping processes. They can be attributed to the charge-trapping phenomenon<sup>19</sup> initially discovered by Murray and co-workers<sup>20,21</sup> on bilayer films of redox polymers. However, they disappeared when the cyclic voltammetry was performed in uniquely n- (0 to –1.5 V) or p-doping (0 to 0.8 V) regions. If the potential

(18) Bard, A. J.; Faulkner, L. R. *Électrochimie. Principes, méthodes et applications (Electrochemistry: Principles, methods and applications)*; Masson: Paris, 1983.

(19) Zotti, G.; Schiavon, G.; Zecchin, S. *Synth. Met.* **1995**, *72*, 275.

(20) Abruna, H. D.; Denisevich, P.; Umana, M.; Meyer, T. J.; Murray, R. W. *J. Am. Chem. Soc.* **1981**, *103*, 1.

(21) Denisevich, P.; Willman, K. W.; Murray, R. W. *J. Am. Chem. Soc.* **1981**, *103*, 4727.

cycling is performed in the potential range encompassing only the prepeaks, these are maintained with a reversible charge exchange.<sup>19</sup> As was already shown for polyphenylthiophenes,<sup>22</sup> we observed that the size of the prepeaks was dependent on the current density used for polymer growth. These prepeaks will be further investigated below using electrochemical impedance spectroscopy.

From the data of Figure 1, a band gap of about 1.2 eV was calculated from the difference between the threshold potentials for p- and n-doping. This value is similar to that already reported for PCDT.<sup>7,12,14</sup> Our polymer can be cycled between the n- and p-doping states over a potential window of about 2 V. Thus, a cell voltage of about 2 V for an electrochemical supercapacitor based on PCDT as active material for both electrodes becomes possible.<sup>2,3</sup>

Table 1 reports the voltammetric charge for the anodic,  $Q_{ox(p)}$  and cathodic,  $Q_{red(p)}$ , branches of the p-doping wave, the cathodic,  $Q_{red(n)}$  and anodic,  $Q_{ox(n)}$ , branches of the n-doping process, and the doping levels corresponding to  $Q_{ox(p)}$  and  $Q_{red(n)}$ . No definitive trend can be seen from the variation in the voltammetric charge when the growth conditions are changed. Nonetheless, we decided to use 20 mM CDT, 0.5 mA/cm<sup>2</sup> as our standard conditions as they yielded a ratio of p- and n-doping voltammetric charges which is the closest to unity. These conditions were used to prepare the electrodes for the galvanostatic cycling experiments (vide infra). The ratio of doping–dedoping charges is always larger than unity and an average value of about 0.5 can be calculated from the data of Table 1. This charge ratio is lower than those found for poly(3-phenylthiophene) derivatives<sup>23</sup> and suggests that some irreversible processes might be occurring during potential cycling. The later can be invoked to explain the initial performance losses of PCDT-based capacitor (vide infra). Doping levels of 0.19 and 0.21 can be estimated for p- and n-doped states for the film grown in the standard conditions by assuming a polymerization efficiency of 100%. It is clear that these doping levels are underestimated since the polymerization efficiency is presumably lower than 100%. In our case, the polymerization efficiency has been roughly estimated to 80% for a 5 C/cm<sup>2</sup> film grown on carbon paper. Moreover, polymerization efficiencies of about 70% have also been recently reported for other polythiophene derivatives.<sup>23</sup> It is also interesting to compare the relative amount of polymer that can be electrochemically addressed (in our case it is equivalent to the doping level) with that of others polymers. Thus, the  $Q_{ox(p)}/Q_{dep}$  (or  $Q_{red(n)}/Q_{dep}$ ) ratio is ranging from 10 to 20%, in agreement with values reported in the literature for polyphenylthiophene.<sup>23–25</sup>

### Electrochemical Impedance Spectroscopy, EIS.

EIS was used to evaluate the low-frequency capacitance as well as the ionic and electronic resistance of the polymer electrode. Figure 2 shows the complex imped-

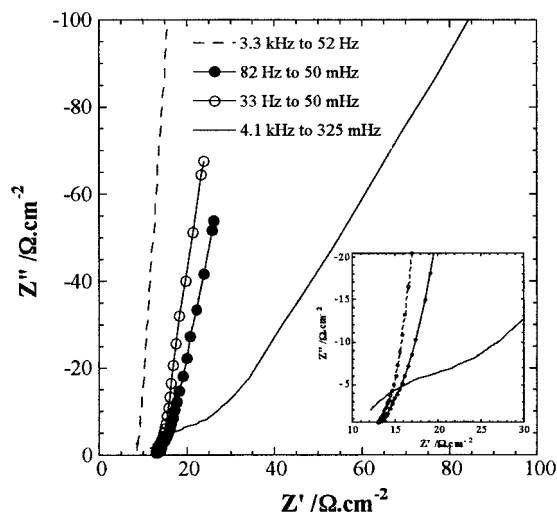


**Figure 2.** Complex plane impedance plots for bare carbon paper, CP, electrode at open circuit potential (---) and PCDT film coated CP electrodes at  $-1.3$  V (●);  $0.5$  V (○);  $0$  V (—) in  $1$  M  $\text{Et}_4\text{NBF}_4/\text{acetonitrile}$  solution. Growth conditions:  $20$  mM CDT,  $0.1$  mA/cm<sup>2</sup>;  $Q_{deposited} = 1$  C/cm<sup>2</sup>. (Inset) High-frequency data: (●)  $82$ – $130$  mHz, (○)  $33$ – $163$  mHz, (—)  $4.1$ – $10$  Hz.

**Table 2. Electrochemical Impedance Spectroscopy Parameters for PCDT<sup>a</sup>**

electrode potential (V vs Ag/Ag <sup>+</sup> )	$C_{LF}^b$ (mF/cm <sup>2</sup> )	$R_H^c$ (Ω)	$R_W^d$ (Ω)	$R_L^e$ (Ω)	$R_l^f$ (Ω)	$R_l^g$ (Ω)	$R_l^h$ (Ω)	$R_e$ (Ω)
-1.5	58	12	12.5	14	19	6	10	7
-1.4	60	13	13	15	27	6	13	7
-1.3	62	13	13	15	25	6	13	7
-1.2	41	13	13	16	26	9	16	6
-1.0	7	9	20	38	175	87	75	14
0	8	12	17	19	204			
0.1	13	12	13.5	14	43			
0.2	22	12	13	13.5	21			
0.3	32	12	12.5	14	20	6	10	7
0.4	42	13	13	14	15	3	5	0.3
0.5	48	13	13	14	16	3	5	0.3
0.6	47	13	13	14	21	3	5	0.3
0.7	39	12	13	14	18	6	5	0.3
0.8	30	12	13	13.5	20	5	5	0.3

<sup>a</sup> Growth conditions of PCDT: deposited charge  $1$  C/cm<sup>2</sup>,  $20$  mM CDT and  $i = 0.1$  mA/cm<sup>2</sup>. <sup>b</sup> Low-frequency capacitance. <sup>c</sup> High-frequency intercept. <sup>d</sup> Warburg region intercept. <sup>e</sup> Low-frequency intercept. <sup>f</sup> Ionic resistance (Randles/Warburg diffusion).  $Z^2 = R_l / 2\pi f C_{LF}$  where  $Z^2$  is  $Z'^2 + Z''^2$  and  $f$  is frequency. <sup>g</sup> Ionic resistance,  $R_e = 0$  (linear transmission line model).  $R_l = 3(R_L - R_H)$  with  $R_H = R_s$ . <sup>h</sup> Ionic resistance (linear transmission line model).  $(R_W - R_s)^{-1} = R_e^{-1} + R_l^{-1}$  and  $(R_L - R_s) = R_e + R_l$  with  $R_s = 8.5$  Ω and  $R_W =$  Warburg diffusion line intercept with real impedance axis. <sup>i</sup> Electronic resistance (linear transmission line model).  $(R_W - R_s)^{-1} = R_e^{-1} + R_l^{-1}$  and  $(R_L - R_s) = R_e + R_l$  with  $R_s = 8.5$  Ω and  $R_W =$  Warburg diffusion line intercept with real impedance axis.

ance plots ( $Z''$  vs  $Z'$ ) for a bare carbon paper electrode at open circuit potential and PCDT-coated carbon paper electrodes in the oxidized, neutral, and reduced states. For both the oxidized form ( $E = 0.5$  V) and the reduced form ( $E = -1.3$  V), the high-frequency data form a straight line with a 45° angle and the low-frequency data lie on an almost vertical line. The later correspond to the behavior of a capacitor. The high-frequency intercepts,  $R_{HS}$ , of the polymer coated electrode are given as a function of the electrode potential in Table 2. The projected length of the 45° Warburg-type line on the real impedance axis characterizes the slow ion migration process in the solution pores.<sup>22</sup> At low fre-

(22) Guerrero, D. J.; Ren, X.; Ferraris, J. P. *Chem. Mater.* **1994**, *6*, 1437.

(23) Ferraris, J. P.; Eissa, M. M.; Brotherston, I. D.; Loveday, D. C.; Moxey, A. A. *J. Electroanal. Chem.* **1998**, *459*, 57.

(24) Rudge, A.; Raistrick, I.; Gottesfeld, S.; Ferraris, J. P. *Electrochim. Acta* **1994**, *39*, 273.

(25) Gofer, Y.; Killian, J. G.; Sarker, H.; Poehler, T. O.; Searson, P. C. *J. Electroanal. Chem.* **1998**, *443*, 103.

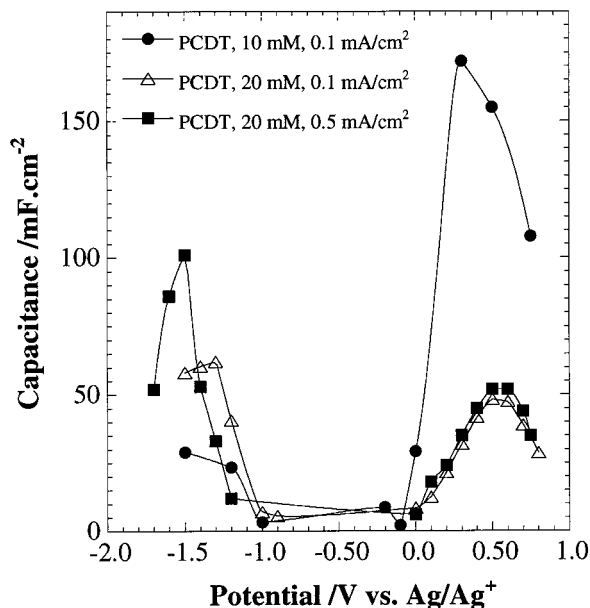


**Figure 3.** Low-frequency capacitance of PCDT ( $Q_{\text{deposited}} = 1 \text{ C/cm}^2$ ) on carbon paper electrodes in 1 M  $\text{Et}_4\text{NBF}_4$  in acetonitrile.

quency, the redox reaction layer encompasses the whole polymer film, which therefore remains in equilibrium with the changing potential. Under these conditions the polymer-coated electrode behaves like a simple capacitor and the complex plane impedance plot becomes almost vertical. The extrapolation of this nearly vertical low-frequency line on the real impedance axis is defined as  $R_L$ .

The capacitance is calculated from the slope of a plot of the imaginary component of the impedance, at low frequency, as a function of the reciprocal of the frequency.<sup>26</sup> Figure 3 depicts the variation in the low frequency capacitance with electrode potential for various growth conditions. The shapes of these plots correlate well with those of the corresponding cyclic voltammograms except that the intensity of the low frequency capacitance prepeaks is significantly smaller than that of the prepeaks of the CV (Figure 1). This is an important result which confirms that most of the charge associated with the prepeaks of the CV is trapped charge.<sup>20,27–31</sup> The trapped charge cannot be detected by EIS because the polymer electrode is polarized for some time prior to the measurements. This is sufficient to release the trapped charge. The remainder of the prepeak charge of the CV gives rise to the small prepeak of the capacitance–potential plot and is attributed to the degradation of the polymer<sup>19</sup> or a resistive effect due to the polymer low electronic conductivity.<sup>32</sup> The capacitance for the p-doping process can reach values as high as  $200 \text{ mF/cm}^2$  and similar

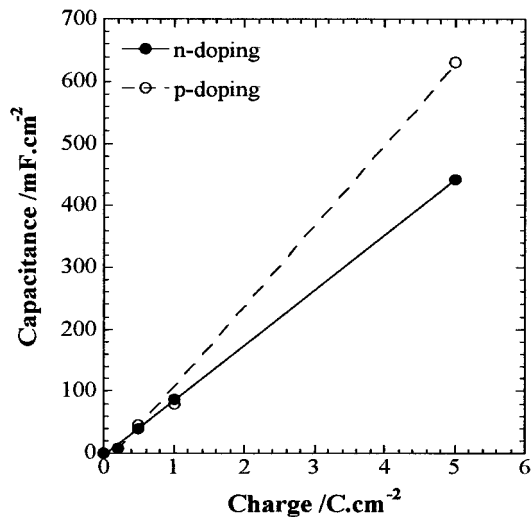


**Figure 4.** Low-frequency capacitance as a function of polymer deposition charge.

capacitances can also be achieved for the two doping states for specific growth conditions of the polymer film. Indeed, low-frequency capacitances of  $\sim 60 \text{ mF/cm}^2$  ( $\sim 70 \text{ F/g}$  with  $\Delta m_{\text{polymer}} = 0.0009 \text{ g}$ ) were achieved when a poly(CDT) film was grown from a 20 mM CDT solution at a current density of  $0.1 \text{ mA/cm}^2$  (see Figure 3). An interesting situation would occur if the capacitance for both the n- and p-doped states were similar because, in this case, the same amount of polymer would be deposited for both the positive and the negative electrodes of an electrochemical capacitor. This would also enable a reversal in the polarity of the electrodes of the supercapacitor. A linear increase of the low-frequency capacitance with deposited charge (film thickness) as shown in Figure 4 is attractive as high polymer loading is required to increase the energy density of a practical supercapacitor. This would require that the relative fraction of the polymer which is electrochemically addressed does not change with film thickness within the range investigated in this study. Further, the thicker film ( $5 \text{ C/cm}^2$ ) displayed a lower n-doping low-frequency capacitance ( $98 \text{ F/g}$ ) as compared to the p-doping  $C_{LF}$  ( $142 \text{ F/g}$ ). This effect might be attributed to a slower ionic transport rate through the n-doped polymer film.<sup>23</sup>

Both the linear transmission line model<sup>33–37</sup> and the Randles equivalent circuit<sup>38,39</sup> have been widely used to analyze the impedance data of electronically conducting polymers. Table 2 provides representative values of ionic ( $R_i$ ) and electronic ( $R_e$ ) resistances for a PCDT film as a function of electrode potential. We have used three approaches to evaluate the ionic resistance of the film so as to investigate the effect of potential on the ionic resistance of the polymer for both the p- and n-doped states. One of these was to calculate the ionic resistance using the Warburg region of the impedance spectrum

(26) Fiordiponti, P.; Pistoia, G. *Electrochim. Acta* **1989**, *34*, 215.

(27) Denisevich, P.; Abruna, H. D.; Leider, C. R.; Meyer, T. J.; Murray, R. W. *Inorg. Chem.* **1982**, *21*, 2153.

(28) Berthelot, J. R.; Angely, L.; Delaunay, J.; Simonet, J. *New J. Chem.* **1987**, *11*, 487.

(29) Crooks, R. M.; Chyan, O. M.; Wrighton, M. S. *Chem. Mater.* **1989**, *1*, 2.

(30) Borjas, R.; Buttry, D. A. *Chem. Mater.* **1991**, *3*, 872.

(31) Zhou, Z.; Maruyama, T.; Kanbara, T.; Ikeda, T.; Ichimura, K.; Yamamoto, T.; Tokuda, K. *J. Chem. Soc., Chem. Commun.* **1991**, 210.

(32) Gottesfeld, S.; Redondo, A.; Rubinstein, I.; Feldberg, S. W. *J. Electroanal. Chem.* **1989**, *265*, 15.

(33) Ren, X.; Pickup, P. G. *J. Chem. Soc., Faraday Trans.* **1993**, *89*, 321.

(34) Ren, X.; Pickup, P. G. *J. Phys. Chem.* **1993**, *97*, 5356.

(35) Pickup, P. G. *J. Chem. Soc., Faraday Trans.* **1990**, *86*, 3631.

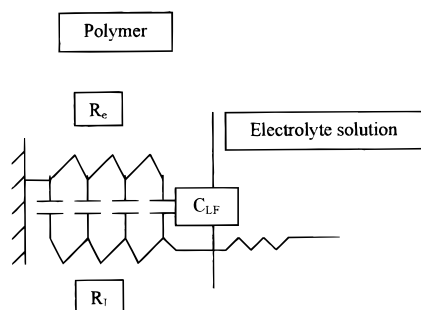
(36) Ren, X.; Pickup, P. G. *J. Electrochem. Soc.* **1992**, *139*, 2097.

(37) Duffitt, G. L.; Pickup, P. G. *J. Chem. Soc., Faraday Trans.* **1992**, *88*, 1417.

(38) Komura, T.; Sakabayashi, H.; Takabashi, K. *Bull. Chem. Soc. Jpn.* **1995**, *72*, 476.

(39) Osaka, T.; Nakajima, T.; Shiota, K.; Momma, T. *J. Electrochem. Soc.* **1992**, *138*, 2853.

Scheme 1



for the polymer in both conducting states by plotting  $Z^2$  as a function of the reciprocal of the frequency. Another involved the evaluation of the ionic resistance using the transmission line model (see Scheme 1). This method requires knowledge of the solution resistance ( $R_s$ ). Two ways may be used to evaluate this resistance. One uses a high-frequency intercept measured with a bare carbon paper electrode at open circuit potential and the other considers the high-frequency intercept,  $R_H$ , of the PCDT coated carbon paper electrode. The latter assumes that the electronic resistance is negligible, as might be expected for conducting states of the polymer and, in this case,  $R_i$  can be computed from  $R_i = 3(R_L - R_H)$ . On the other hand, by using the high-frequency intercept, as for the former, measured at a bare carbon paper electrode ( $R_s = 8.5 \Omega$ ), it is possible to evaluate the ionic and electronic resistances. These values are summarized in Table 2. Table 2 also shows that  $R_i$  values evaluated from the Randles analysis are systematically higher than those obtained by the linear transmission line in agreement with other workers.<sup>33,37</sup> We believe that the discrepancy is due to an underestimation of the low-frequency intercept ( $R_L$ ) which leads to smaller  $R_i$  values when evaluated by the linear transmission line model.

Table 2 clearly indicates that the ionic resistances of the n-doped state are slightly higher than those of the p-doping process as has already been observed for other polythiophene derivatives.<sup>22,23</sup> This is attributed to the slower transport of cation ( $\text{Et}_4\text{N}^+$ ) in the n-doped polymer relative to the anion ( $\text{BF}_4^-$ ) in the p-doped polymer. The ionic and the electronic resistances for both the n- and p-doping states between  $-1.2$  and  $-1.5$  V, and  $0.1$  and  $0.7$  V, respectively remain quite constant. However, at the onset of either the p- or the n-doping processes at  $0$  and  $-1$  V, respectively the ionic resistance increases. The use of two methods to evaluate  $R_i$  deserves some comment. Since the electronic resistance of conducting polymers is usually very low, the calculation of  $R_i$  by letting  $R_e = 0$  is probably the more appropriate method. However, it is difficult to rule out completely the second method. Further, in the middle of the potential range (ca.  $-0.1$  to  $-0.9$  V), the impedance plot showed a semicircle (Figure 2). This is usually attributed to a series combination of a charge-transfer resistance and a double layer capacitance,<sup>40</sup> and it will not be discussed any further here.

**Scanning Electron Microscopy.** Photomicrographs were obtained for polymer films grown on carbon paper and on a platinum electrode, and both show an open

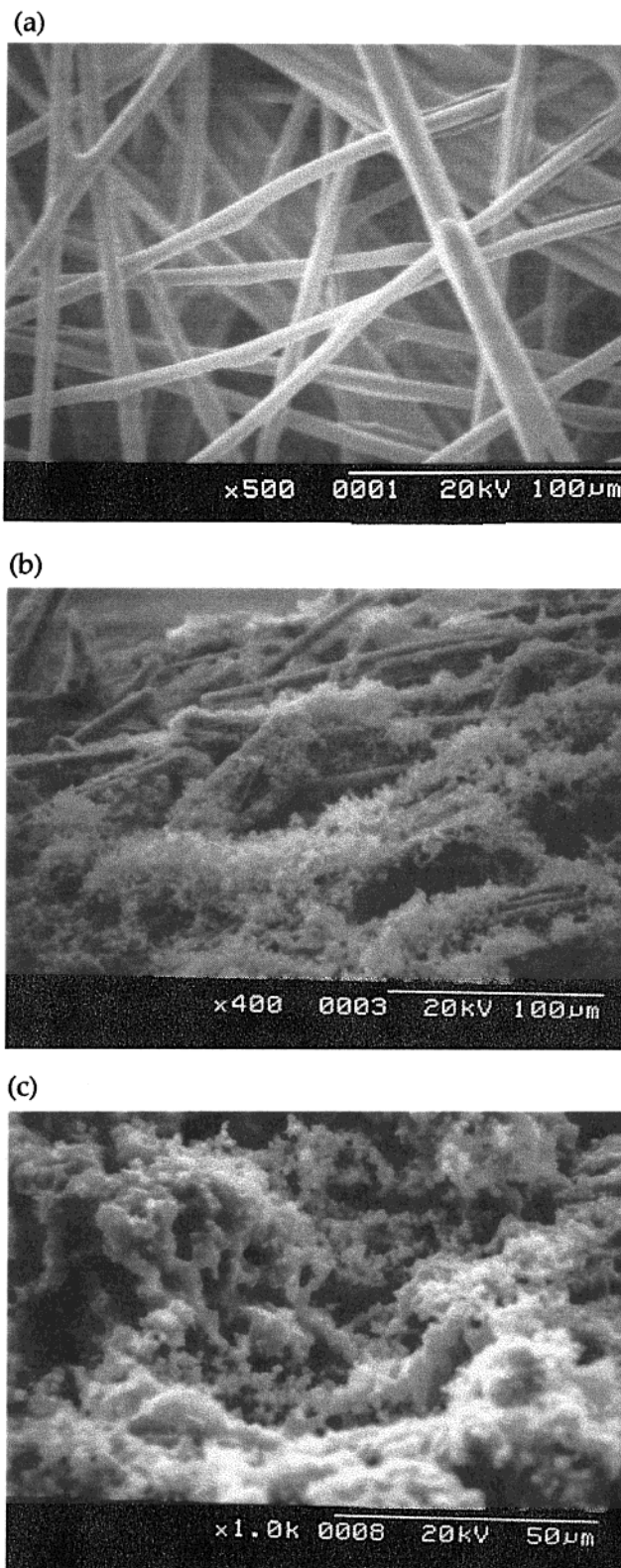


**Figure 5.** Scanning electron micrographs of (a) a carbon paper electrode, (b) a PCDT film grown on carbon paper, and (c) a PCDT film grown on a platinum electrode.  $Q_{\text{deposited}} = 1 \text{ C/cm}^2$ .

and rough morphology for the PCDT film (Figure 5). Figure 5a also shows a photomicrograph for a bare carbon paper electrode and is characterized by carbon fibers with about a  $10 \mu\text{m}$  diameter. In contrast to the platinum electrode (Figure 5c), the carbon paper fibers (Figure 5b) do not seem to be completely coated at a similar deposition charge, indicating that a higher

(40) Ren, X.; Pickup, P. G. J. *Electroanal. Chem.* **1997**, *420*, 251.

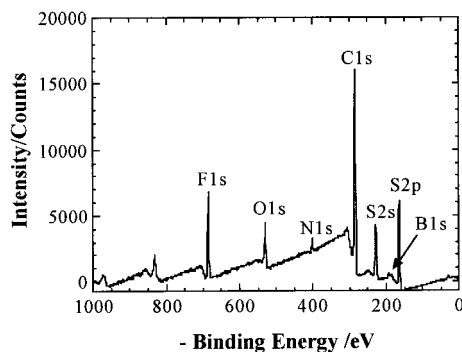


**Figure 6.** XPS survey scan of Pt-supported PCDT film. Growth conditions: 20 mM CDT, 1 M  $\text{Et}_4\text{NBF}_4$ /acetonitrile, 0.5 mA/cm<sup>2</sup>;  $Q_{\text{deposited}} = 1 \text{ C/cm}^2$ .

**Table 3. Surface Elemental Analyses of PCDT**

samples	elemental composition <sup>a</sup> determined by XPS
as grown ( $E_{\text{stabilization}} = 0.73 \text{ V}$ )	$\text{C}_9\text{O}_{0.5}\text{S}_2$
reduced ( $-1.4 \text{ V}$ )	$\text{C}_9\text{O}_1\text{S}_2$
oxidized ( $+0.4 \text{ V}$ )	$\text{C}_{4.5}\text{O}_{0.5}\text{S}_2$
neutral (cycled, stopped at $-0.5 \text{ V}$ )	$\text{C}_{6.7}\text{O}_{0.7}\text{S}_2$

<sup>a</sup> Average for two experiments.

polymer loading may easily be produced on this type of electrode material. The PCDT film appears as a mat of small globular particles. The relative estimate of the atomic content of the film by EDS indicates a doping level of 0.14 for the oxidized state. The doping level is evaluated from the atomic content of fluorine from the  $\text{BF}_4^-$  anions and sulfur from the PCDT. Since some residual fluorine is detected in the reduced polymer, the doping level for the oxidized sample is calculated from the difference between the fluorine content of the oxidized and reduced films. The resultant value of 0.14 is in fairly good agreement with that obtained from cyclic voltammetry measurements but its accuracy is questionable.

**X-ray Photoelectron Spectroscopy, XPS.** XPS has widely been used to characterize the electronic properties of polymeric materials.<sup>41–44</sup> Figure 6 shows the XPS survey spectrum for neutral PCDT which exhibits the characteristic C 1s at about 285 eV. The S 2p (165 eV) and S 2s (230 eV) peaks are related to the bridged thiophene unit and are observed together with the O 1s peak (530 eV) of the CDT. The peaks at 685, 192, and 401 eV are attributed, respectively, to the fluorine (F 1s), boron (B 1s), and nitrogen (N 1s) of  $\text{Et}_4\text{NBF}_4$  which was used as a supporting electrolyte for the electro-synthesis of PCDT.

XPS core level spectra can be used to determine the surface composition and chemical state of the PCDT polymer for various experimental conditions (Table 3). The elemental compositions are generally in good agreement with the theoretical stoichiometry of the corresponding monomer ( $\text{C}_9\text{O}_1\text{S}_2$  determined by elemental

analysis) except for the oxidized film which curiously shows an excess of sulfur. For the moment, no clear explanation can be invoked to explain this behavior.

The S 2p core level spectra of the PCDT films as grown, in the reduced, oxidized, and neutral (cycled in 1 M  $\text{Et}_4\text{NBF}_4$ /acetonitrile and polarized at  $-0.5 \text{ V}$ ) states are depicted in Figure 7. The deconvolution of the S 2p spectrum was not straightforward due to the presence of various sulfur species (Table 4). These spectra showed a doublet with binding energies of  $163.7 \pm 0.3$  and  $164.9 \pm 0.3 \text{ eV}$  with a full width at half-maximum (fwhm) of  $\sim 1.1 \text{ eV}$  and arose from S 2p spin-orbit coupling (S  $2p_{3/2}$  and S  $2p_{1/2}$ ), with a 2:1 ratio as anticipated.<sup>43</sup> This signal was attributed to the neutral sulfur atoms.<sup>45</sup> A second doublet at  $165.3 \pm 0.4$  and  $166.4 \pm 0.5 \text{ eV}$  with fwhm of  $\sim 1.6 \text{ eV}$  was assigned to the oxidized sulfur  $\text{S}^{\sigma+}$ .<sup>43,45</sup> In the case of the reduced polymer, the high-energy doublet was observed at slightly higher binding energies. Such an important contribution (about 12%) of the oxidized sulfur species is unexpected and could reflect surface oxidation of the polymer or perhaps the presence of shake up satellite peaks since it is not observed for the neutral polymer. In addition, a peak was observed at lower binding energy and could be deconvoluted into two peaks at 160.1 and 161.4 eV for S  $2p_{3/2}^{\sigma-}$  and S  $2p_{1/2}^{\sigma-}$ , respectively, with a fwhm of about 1.3 eV. By analogy with the oxidized sulfur atoms found in the p-doped polymer, these low binding energy peaks suggest that some sulfur atoms are in a more negatively charged environment. This would be expected for the negative polarons and/or bipolarons which would result from the injection of electrons into the thiophene backbone.<sup>46</sup> A similar low-binding energy signal has recently been observed by our group in the case of n-doped poly(3-phenylthiophene).<sup>47</sup> It is interesting to note that the low-binding energy component was shifted by about  $-3 \text{ eV}$  from that of the neutral sulfur atoms. In contrast, that of the oxidized species was shifted by only  $+1.5 \text{ eV}$  as compared to neutral sulfur atoms. This might be explained by a stronger localization of the negative charges on the sulfur atoms. However, we are currently investigating this phenomenon in more details to gain a better understanding of it and to confirm that this is not an experimental artifact. A low S  $2p^{\sigma-}$  content for the reduced state of the polymer should be noted. This could be explained by the low stability of the negative polarons and the sensitivity of the polymer to trace amounts of oxygen and water.

The doping levels can be evaluated from the S  $2p^{\sigma+}$  or S  $2p^{\sigma-}$  fraction of the S 2p envelope and are presented in Table 5 for PCDT under various experimental conditions. The doping level of the n-doped form was found to be equal to 0.06. From the previous arguments, it seems clear that the n-doping level was underestimated even though some precautions were taken to minimize the polymer's exposure to air and water (see Experimental Section). XPS measurements performed in an electrochemical cell connected to the antichamber of the spectrometer allow for a more easy observation of the

(41) Xing, K. Z.; Fahlman, M.; Chen, X. W.; Inganäs, O.; Salaneck, W. R. *Synth. Met.* **1997**, *89*, 161.

(42) Fabre, B.; Kanoufi, F.; Simonet, J. *J. Electroanal. Chem.* **1997**, *434*, 225.

(43) Ng, S. C.; Fu, P.; Yu, W.-L.; Chan, H. S. O.; Tan, K. L. *Synth. Met.* **1997**, *87*, 119.

(44) Xing, K. Z.; Fahlman, M.; Lögdlund, M.; Berggren, M.; Inganäs, O.; Andersson, M. R.; Boman, M.; Stafström, S.; Iucci, G.; Bröms, P.; Johansson, N.; Salaneck, W. R. *Synth. Met.* **1996**, *80*, 59.

(45) Kang, E. T.; Neoh, K. G.; Tan, K. L. *Phys. Rev. B* **1991**, *44*, 10461.

(46) *Handbook of organic conductive molecules and polymers*; Nalwa, H. S., Ed.; John Wiley & Sons Ltd.: New York, 1997; Vol. 3, p 709.

(47) Naudin, E.; Bélanger, D.; Guay, D. Work in progress.

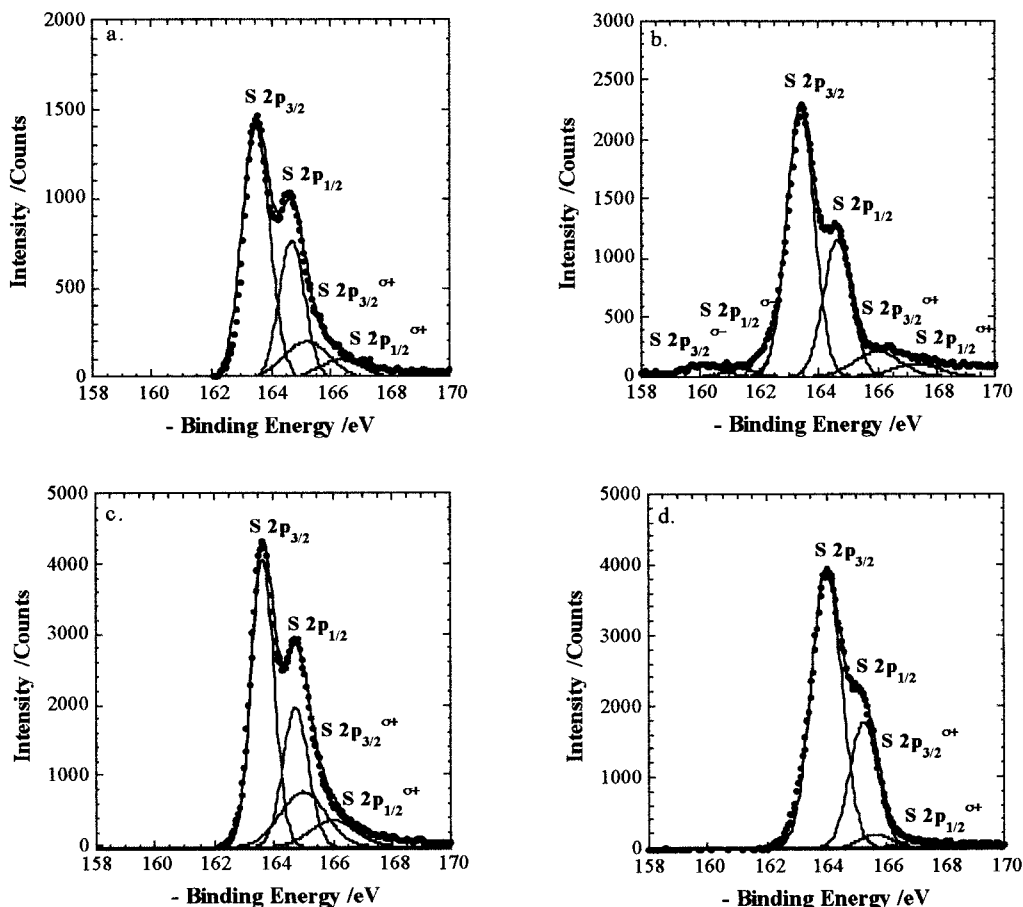


**Figure 7.** XPS S 2p spectra of PCDT films: (a) as grown, (b) reduced, (c) oxidized, and (d) neutral state in 1 M Et<sub>4</sub>NBF<sub>4</sub>/acetonitrile.

**Table 4. S 2p Deconvolution Parameters of PCDT**

S 2p	S 2p <sub>3/2</sub> <sup>σ<sup>-</sup></sup>		S 2p <sub>1/2</sub> <sup>σ<sup>-</sup></sup>			S 2p <sub>3/2</sub>		S 2p <sub>1/2</sub>			S 2p <sub>3/2</sub> <sup>σ<sup>+</sup></sup>		S 2p <sub>1/2</sub> <sup>σ<sup>+</sup></sup>		
	E <sub>B</sub> (eV)	FWHM	E <sub>B</sub> (eV)	FWHM	%	E <sub>B</sub> (eV)	FWHM	E <sub>B</sub> (eV)	FWHM	%	E <sub>B</sub> (eV)	FWHM	E <sub>B</sub> (eV)	FWHM	%
as grown						163.5	1.1	164.7	1.0	81	165.2	1.8	166.3	1.8	19
reduced	160.1	1.4	161.4	1.2	6	163.4	1.1	164.6	1.1	82	166.0	1.8	167.3	1.8	12
oxidized						163.7	0.9	164.8	1.0	73	165.0	1.8	166.0	1.8	27
neutral						164.0	1.2	165.3	1.1	95	165.7	1.2	167.0	1.3	5

**Table 5. Chemical Composition of PCDT for Various Experimental Conditions**

samples	doping level	N/S	F/S	F/N
as grown (E <sub>stabilization</sub> = 0.73 V)	(S 2p) <sup>σ<sup>+</sup></sup> /(S 2p) 0.19	0.42	0.45	4.3
reduced (-1.4 V)	(S 2p) <sup>σ<sup>-</sup></sup> /(S 2p) 0.06	0.33	0.20	2.0
oxidized (+0.4 V)	(S 2p) <sup>σ<sup>+</sup></sup> /(S 2p) 0.27	0.04	0.05	5.0
neutral	(S 2p) <sup>σ<sup>+</sup></sup> /(S 2p) 0.05	0.05	0.06	4.9

S 2p<sup>σ<sup>-</sup></sup> form of the reduced state as such measures would avoid the reoxidation of the polymer.<sup>47</sup> As expected, the neutral form of the polymer displays a low doping level of 0.05. Some residual oxidized sulfur atoms must be present in the neutral polymer but at a significantly lower level than in either the as-grown or oxidized PCDT. For these two polymer electrodes, doping levels of 0.19 and 0.27, respectively, were determined. The doping level for the oxidized state obtained by XPS with the S 2p data (0.27) was higher than the doping levels found by cyclic voltammetry (0.19) and EDAX (0.14). However, by taking into account a polymerization efficiency of 80% (vide supra), a doping level of 0.23 is obtained by CV, which is more consistent with that found by XPS.

The doping level can also be calculated using *F/S* and *N/S* ratios since the oxidized sites of the PCDT would be compensated by the BF<sub>4</sub><sup>-</sup> anions, whereas the Et<sub>4</sub>N<sup>+</sup> cations would act as dopants for the reduced form of the polymer. The doping level values determined by this method are included in Table 5. Surprisingly, these doping levels do not match with those measured by deconvolution of the S 2p core level spectra. The higher values for the as-grown polymer (*F/S* = 0.45) and the n-doped polymer (*N/S* = 0.33) can be attributed to an excess of the salt Et<sub>4</sub>NBF<sub>4</sub> within the polymer. On the other hand, the lower doping level for the p-doped polymer cannot readily be explained but might be related to the inexact elemental composition evaluated by XPS (see Table 3). For the neutral state, the *N/S* and *F/S* ratios should be almost zero since the polymer should not contain any ionic species. This was not the case since some salt may have been trapped in the polymeric film.

The C 1s core level spectra for the PCDT in various states are shown in Figure 8. The C 1s envelope is deconvoluted into three components (Table 6). The main peak at 284.5 eV can be attributed to the contribution



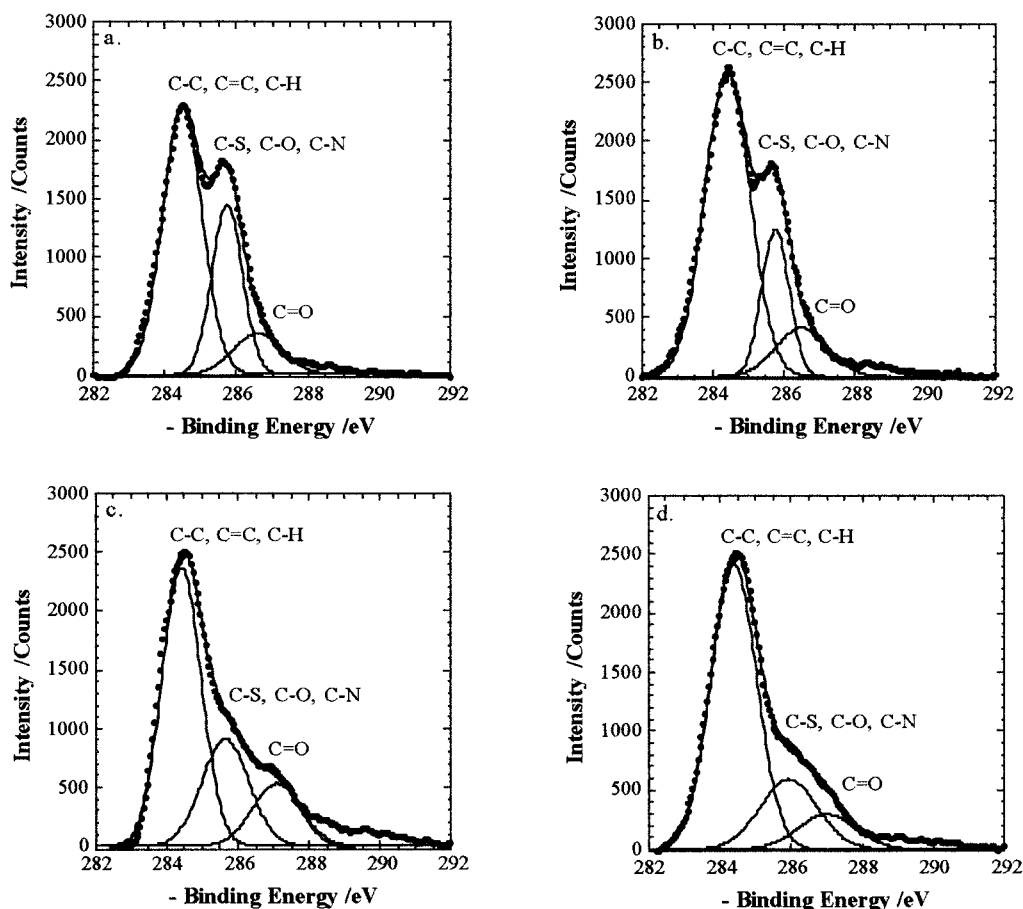


**Figure 8.** XPS C 1s spectra of PCDT films: (a) as grown, (b) reduced, (c) oxidized, and (d) neutral state in 1 M Et<sub>4</sub>NBF<sub>4</sub>/acetonitrile.

**Table 6. C 1s Deconvolution Parameters of PCDT**

C1s	C-C C=C C-H			C-S C-O C-N			C=O		
	$E_B$ (eV)	%	FWHM	$E_B$ (eV)	%	FWHM	$E_B$ (eV)	%	FWHM
as grown	284.5	60	1.3	285.8	29	1	286.6	11	1.6
reduced	284.5	68	1.5	285.8	20	0.9	286.5	12	1.7
oxidized	284.5	57	1.3	285.7	27	1.6	287.1	16	1.6
neutral	284.5	68	1.5	285.9	21	1.9	287.0	11	1.9

**Table 7. O 1s Deconvolution Parameters of PCDT**

O 1s	$E_B$ (eV)	%	FWHM	C=O			C-O			H <sub>2</sub> O		
				$E_B$ (eV)	%	FWHM	$E_B$ (eV)	%	FWHM	$E_B$ (eV)	%	FWHM
as grown	530.0	29	1.9	531.3	56	1.5	532.7	31	1.6	535.2	13	2.8
reduced				531.3	45	1.6	532.9	18	1.7	535.2	8	2.8
oxidized				531.4	57	1.3	532.6	26	1.3	535.1	17	2.8
neutral				531.6	46	1.6	532.7	22	1.7	535.4	17	2.8

of C-C, C=C, and C-H.<sup>42,43</sup> The peak signal at ~285.8 eV was assigned to C-S, C-O, and C-N,<sup>42,43</sup> and the third peak centered at 286.5–287.1 eV is indicative of the presence of C=O.<sup>43,48</sup> The position of this peak seems to shift with the oxidation state of the polymer. Recent IR data show a shift of the C=O band to a higher wavenumber upon oxidation, indicating a net increase in the positive charge on the carbon atom of the carbonyl group<sup>15</sup> but our XPS results do not show the same trend. Nonetheless, the slight shift to a lower binding energy

observed for the n-doped polymer is in agreement with recent IR data.<sup>15</sup> However, some caution should be taken with the preceding interpretation because of shake up satellite peaks present in the high binding energy region of the C 1s core level spectrum.

Finally, three peaks (Table 7) were commonly deconvoluted in the O 1s core level spectra (Figure 9) of the polymers for C=O (~531.4 eV), C-O (~532.7 eV), and adsorbed H<sub>2</sub>O (~535.2 eV).<sup>43,49</sup> The presence of other forms of water (e.g., Chemisorbed, bound) can also contribute to the O 1s signal at binding energies

(48) Moulder, J. F.; Stickle, W. F.; Sobol, P. E.; Bomben, K. D. *Handbook of X-ray Photoelectron Spectroscopy*; Chastain, J., Ed.; Perkin-Elmer Corporation: Eden Prairie, MN, 1992.

(49) Ilangoan, G.; Chandrasekara Pillai, K. *Langmuir* **1997**, *13*, 566.

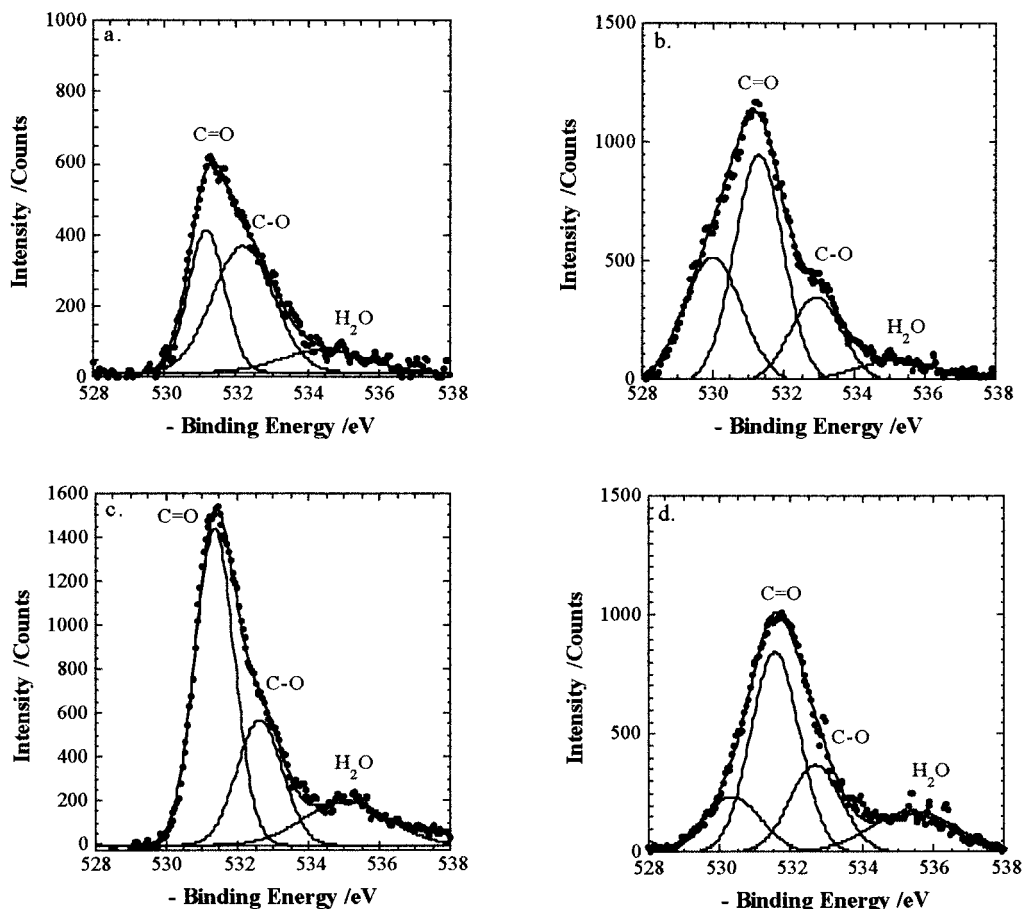


**Figure 9.** XPS O 1s spectra of PCDT films: (a) as grown, (b) reduced, (c) oxidized, and (d) neutral state in 1 M  $\text{Et}_4\text{NBF}_4$ /acetonitrile.

between 532 and 533.7 eV.<sup>49</sup> In addition the O 1s spectra of the reduced and neutral states showed a fourth peak. This peak, located at  $\sim 530.2$  eV, was quite clear and it indicated a net decrease in the negative charge on the oxygen atom. It has already been shown that electrolyte impurities and oxygen may affect the stability of the conducting polymers under electrochemical conditions.<sup>50,51</sup> Indeed, the polymer might bear a S=O functionality on a few monomer units due to chemical degradation. This process is considerably quicker in the presence of nucleophilic additives, solvents such as  $\text{H}_2\text{O}$  and supporting electrolytic anions such as  $\text{BF}_4^-$ .<sup>50</sup> However, it is very unlikely that this S=O would give rise to a peak at such low binding energy (530.2 eV). Due to their similar electronegativities, C and S bonded to oxygen should show a O 1s peak with similar binding energy. This is confirmed by XPS data of sulfonated polymer for which the O 1s peak at 531.7 eV is attributed to the  $\text{SO}_3\text{H}$  species.<sup>52</sup>

**Galvanostatic Charge/Discharge Cycling.** Constant current charge–discharges at  $2 \text{ mA/cm}^2$  between 0 V and a maximum cell voltage of 2 V were performed on capacitors assembled from PCDT-coated carbon paper electrodes in 1 M  $\text{Et}_4\text{NBF}_4$  in acetonitrile. Representative cycling curves are displayed in Figure 10. The stability of a PCDT-based electrochemical super-

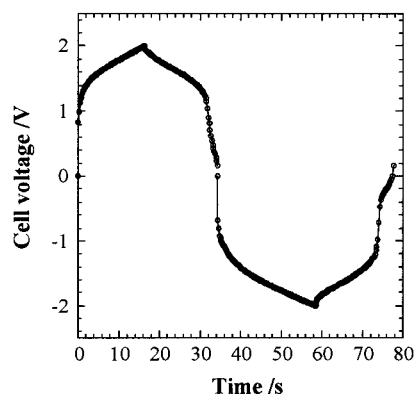


**Figure 10.** Variation of the cell voltage with time during constant current ( $2 \text{ mA/cm}^2$ ) cycling of a PCDT capacitor (two electrodes). Electrolyte: 1 M  $\text{Et}_4\text{NBF}_4$  in acetonitrile.

capacitor upon cycling has been evaluated and the variation of the discharge capacity with the number of cycles is given in Figure 11. A decrease from 35 to 10  $\text{mC/cm}^2$  was observed during the first 20 cycles but then the discharge capacity remained constant for the next 80 cycles. The decrease might be attributed to irreversible degradation of a fraction of the polymer in the initial charge–discharge cycles as suggested by the unbalanced doping–dedoping charge ratio of the CVs (vide supra). It should be noted that the cycling was actually performed between  $-2$  and  $2$  V which, since each polymer electrode is scanned between the p- and n-doped states, is equivalent to a cyclic voltammetry experiment performed over the complete range of electroactivity of the

(50) Pud, A. A. *Synth. Met.* **1994**, *66*, 1.

(51) Barsch, U.; Beck, F. *Electrochim. Acta* **1996**, *41*, 1761.

(52) Idage, S. B.; Badrinarayanan, S. P.; Vernekar, S. P.; Sivaram, S. *Langmuir* **1996**, *12*, 1018.

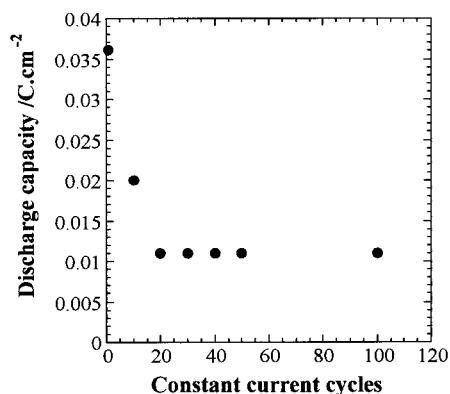


**Figure 11.** Variation of the discharge capacity with the number of constant current cycles at a current density of 2 mA/cm<sup>2</sup> and for cell potentials between 0 and 2 V.  $Q_{\text{deposited}} = 1 \text{ C/cm}^2$ . Electrolyte: 1 M Et<sub>4</sub>NBF<sub>4</sub> in acetonitrile.

polymer. This cycling procedure was used instead of the more conventional method, which consists of cycling between 0 and an appropriate cell voltage, to determine if an inversion of the polarity of the capacitor would be beneficial. Before cycling, the potential of each electrode is usually set at ca.  $-0.2 \text{ V}$  vs Ag/Ag<sup>+</sup>. This is about halfway between the positive and negative limits of the CV (see Figure 1). During the charge process, the potential limit of the positive electrode was about  $0.5 \text{ V}$  vs Ag/Ag<sup>+</sup> and the negative electrode reached a value near that of  $-1.5 \text{ V}$  vs Ag/Ag<sup>+</sup>. A discharge capacity of 6 (mA h)/g of electroactive polymer (0.0018 g) was calculated from the discharge curve. This is only 2% of the theoretical charge capacity of PCDT, which may be evaluated at 280 (mA h)/g, but the value compares well with the specific discharge capacity values found for poly 3-(phenylthiophene) derivatives by Ferraris and al.<sup>53</sup>

Two of the important parameters of a capacitor besides its discharge capacity is its energy density and its charge cycle efficiency. The latter, defined as the ratio of the energy delivered by the capacitor upon discharge to the energy needed to charge it, is close to 100%.<sup>25</sup> The energy density for a PCDT capacitor is 6 (W h)/kg of active material (with 0.0018 g). Although this is lower than that of poly3-(4-fluorophenyl)thiophene (PFPT)-based device,<sup>25,53</sup> the energy density for the PCDT-based capacitor is similar to that of the symmetric poly(dithienothiophene) (PDTT)-based supercapacitor.<sup>54,55</sup> The power density computed from the data of Figure 10 is 1 (kW)/kg of active material of the capacitor for a discharge time of 18 s. The power density exhibited by a PCDT-based device, for a discharge

current of 2 mA/cm<sup>2</sup>, is comparable to PFPT at a discharge current of 10 mA/cm<sup>2</sup>.<sup>53</sup> A similar power density was also reported by Arbizzani and al.<sup>54,55</sup> for a type III PDTT supercapacitor with a comparable discharge time. The midterm requirements established by the U. S. Department of Energy, DOE, for supercapacitors ( $E > 5 \text{ (W h)/kg}$  and  $P > 500 \text{ W/kg}$ , including electrolyte, separator, etc.) can be met by a PCDT-based supercapacitor which is therefore an attractive polymer-based supercapacitor device even if it remains clear that additional work is required to improve the stability of the PCDT based capacitors and at least maintain the initial discharge capacity value.

## Conclusion

Electrochemical and physical characterizations of the PCDT-coated carbon paper electrodes were performed. From the cyclic voltammetry data, a band gap value of about 1.2 eV with an electroactivity window of 2 V were computed. In its conducting states, the PCDT-coated electrode behaves like a capacitor, and the corresponding complex plane impedance plot becomes almost vertical. A low-frequency capacitance of about 70 F/g (deposited charge = 1 C/cm<sup>2</sup>) was determined for both the p- and n-doped states. This low-frequency capacitance increases with film thickness. SEM micrographs of PCDT showed an open and rough morphology. For the n-doped polymer, XPS measurements allowed the observation of sulfur atoms in a more negatively charged environment attributed to S 2p<sup>σ-</sup>. Capacitors assembled from PCDT-coated carbon paper electrodes showed a decrease in the discharge capacity during the first 20 cycles but thereafter it remained constant. It is clear that the stability of such a device has to be improved. The corresponding energy,  $E$ , and power,  $P$ , densities were found to be, respectively, 6 (W h)/kg and 1 kW/kg of active material (0.0018 g) for a discharge time of 18 s and meet the DOE requirements for supercapacitors ( $E > 5 \text{ (W h)/kg}$  and  $P > 500 \text{ W/kg}$ ). However, it should be kept in mind that energy and power densities should be scaled down by a factor of 2–5 depending on the composition (electrolyte, solvent) and packaging (current collector, casing) of the practical supercapacitor.

**Acknowledgment.** This research was funded by the National Science and Engineering Research Council through a strategic grant (to L.B. and D.B.) and an equipment grant for an XPS spectrometer (to D.B. and nine others). We also acknowledge the financial contribution of UQAM. We thank R. Mineau from UQAM (Département des Sciences de la Terre) for the SEM measurements. The technical assistance of G. Veilleux of INRS-Énergie et Matériaux for the XPS measurements is also appreciated.

CM990129B

(53) Ferraris, J. P.; Eissa, M. M.; Brotherston, I. D.; Loveday, D. *C. Chem. Mater.* **1998**, *10*, 3528.

(54) Arbizzani, C.; Mastragostino, M.; Meneghello, L. *Electrochim. Acta* **1996**, *41*, 21.

(55) Arbizzani, C.; Mastragostino, M.; Meneghello, L. *Electrochim. Acta* **1995**, *40*, 2223.